PHYSICAL REVIEW D

PARTICLES AND FIELDS

THIRD SERIES, VOL. 2, NO. 11 1 DECEMBER 1970

Measurement of Antiproton-Proton Forward Charge-Exchange Scattering*

W. ATWOOD, B. BARISH, H. W. NICHOLSON, J. PINE, A. V. TOLLESTRUP, AND J. K. YOH
California Institute of Technology, Pasadena, California 91109

AND

A. S. CARROLL
Brookhaven National Laboratory, Upton, New York 11973

AND

F. LOBKOWICZ AND Y. NAGASHIMA†
University of Rochester, Rochester, New York 14627

(Received 27 July 1970)

There is a well-known forward peak in the np forward charge-exchange cross section, for momentum transfers $|t| \lesssim m_\pi^2$. We have performed an experiment to look for analogous behavior in the reaction $\bar{p}p \to \bar{n}n$. The data cover the kinematical region $0 \leq |t| \leq 1.5 m_\pi^2$ at an incident antiproton momentum of 1.80 GeV/c. A forward peak is observed, which is estimated (from results of other experiments) to be considerably smaller than that for np charge exchange. This result can be understood in terms of interference between one-pion exchange and exchange of a particle with even G parity.

I. INTRODUCTION

THE reaction $\bar{p}+p \to \bar{n}+n$, $\bar{p}p$ charge-exchange scattering, can be related to np charge-exchange scattering by arguments based on crossing symmetry[1] and G-parity invariance.[2] The Feynman diagrams in Figs. 1(a) and 1(b) represent the charge-exchange amplitudes, assuming some arbitrary t-channel exchange labeled X. With G invariance, if the left-hand side of the np diagram is operated on with the G-parity operator, the result is the $\bar{p}p$ amplitude multiplied by $-(G_X)$, where G_X is the G parity of the exchanged object. Therefore, the amplitudes for np and $\bar{p}p$ charge exchange are identical for X exchange of odd G parity and opposite in sign for X exchange of even G parity. The difference of the cross sections is therefore sensitive to the interference terms between odd and even G-parity exchanges.

In np charge-exchange experiments a sharp forward peak has been observed for $-t \lesssim m_\pi^2$.[3-6] This experiment is an exploratory look at $\bar{p}p$ charge exchange for this interesting region of momentum transfer, performed as a byproduct of an experiment primarily intended to study $\bar{p}p$ elastic scattering and two-meson annihilations. The idea of the experiment is first to select events in which an antiproton enters a hydrogen target and neither charged particles nor γ rays emerge. For these events, antineutrons which emerge from the target in the forward direction are detected by their interactions in a brass converter. Charged particles resulting from these interactions are observed with wire chambers. Antineutron annihilations are selected by requiring a high multiplicity of charged particles from the converter, including at least one backward particle, and the response of the system to the antineutrons is calibrated with antiprotons.

A bubble-chamber experiment by Hinrichs *et al.*,[7] with antiprotons at a momentum of 1.61 GeV/c, pro-

* Supported in part by the U. S. Atomic Energy Commission. Prepared under Contract No. AT(11-1)-68 for the San Francisco Operations Office, U. S. Atomic Energy Commission.

† Present address: California Institute of Technology, Pasadena, Calif. 91109.

[1] A. Bialas and O. Czyzewski, Phys. Letters **13**, 337 (1964).

[2] R. J. N. Phillips and G. A. Ringland, Phys. Letters **20**, 205 (1966).

[3] R. R. Larsen, Nuovo Cimento **18**, 1039 (1960).

[4] J. L. Friedes, H. Palevsky, R. L. Stearns, and R. J. Sutter, Phys. Rev. Letters **15**, 38 (1965).

[5] G. Manning and A. G. Parham, Nuovo Cimento **41**, 167 (1966).

[6] R. E. Mischke, P. F. Shepard, and T. J. Devlin, Phys. Rev. Letters **23**, 542 (1969).

[7] C. K. Hinrichs, B. J. Moyer, J. A. Poirier, and P. M. Ogden, Phys. Rev. **127**, 617 (1962).

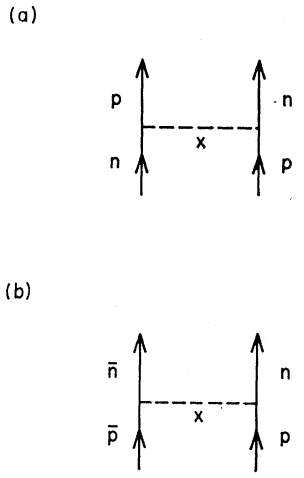

FIG. 1. Feynman diagrams for np and $\bar{p}p$ charge-exchange scattering, with a particle exchange "X."

vides data on the relative cross sections of various processes which can produce forward antineutrons. At this energy, the only significant process, in addition to charge exchange, is single-pion production leading to $\bar{n}p\pi^-$ and $\bar{n}n\pi^0$ final states. Considering the size of the single-pion cross sections and the effectiveness of the veto counters in this experiment, we estimate less than 5% background from reactions other than simple charge exchange. In Sec. II the experimental details are discussed more fully, and the results and interpretation are presented in Sec. III.

II. EXPERIMENTAL METHOD

A. General

The layout of the apparatus, which was originally designed for measuring charged two-body final states with one forward particle and one backward particle,[8] is shown in Fig. 2. A partially separated antiproton beam with momentum 1.80 GeV/c and momentum spread $\pm 2\frac{1}{2}\%$ was used. Antiprotons were identified with a focusing Čerenkov counter, and in tests made with a threshold gas Čerenkov counter, the contamination of pions and muons was found to be less than 1%.

The beam was incident on a 35-cm-long liquid-hydrogen target. As described above, the idea of the experiment was to select events in which neither charged particles nor γ rays emerged from the target, and in which there was an interaction in a converter downstream of the target. Twelve spark chambers were triggered when there was a coincidence between the beam-defining counters upstream of the target and a counter behind the converter, with a number of counters surrounding the target in anticoincidence. The most important of these veto counters are shown in Fig. 2, and each veto counter was preceded by $\frac{1}{4}$ in. of lead to convert γ rays. There was, however, no lead in a small solid angle directly downstream of the target, where it would be traversed by antineutrons headed toward the converter.

The incident antiproton trajectory was measured with wire chambers 1–4, upstream and to the right of the target. For an interaction in the converter which was ascribed to an antineutron originating in the hydrogen target, the angle of the antineutron was determined by comparing the location of the interaction with the extrapolated location and direction of the incident antiproton at the target center. It was required that no particles be observed in chambers 5–8.

The converter was made of brass, $2\frac{1}{2}$ in. thick, in order to provide a high probability for antineutron annihilations and for conversion of π^0 γ rays from the annihilations. The location of an interaction in the converter was inferred from the mean values of the x and y (horizontal and vertical) coordinates of the sparks in wire chamber 11, immediately downstream of the converter. Chamber 10, upstream of the converter, was used to detect backward-going particles. The converter could detect antineutrons making angles between zero and 6° with the beam direction, resulting in a range of four-momentum transfer squared from zero to about $1.5m_\pi^2$.

A field of 20 kG in the magnet served to bend beam particles away from the converter and its associated spark chambers. The probability of the veto counters being struck by a backward particle from an antineutron annihilation was negligible because of the small solid angle and the intervening magnetic field.

B. Calibrations

The assumption underlying the calibrations is that antiproton and antineutron annihilations in the converter occur with equal probabilities and produce identical types of spark distributions in the spark chambers near the converter. Antiproton calibration data were used for three purposes:

(1) to establish criteria which select antiproton or antineutron annihilations and reject γ rays,

(2) to determine for a given criterion an absolute detection efficiency for antiprotons or antineutrons,

(3) to determine for a given criterion the precision with which the coordinates of an annihilation can be determined, and thus to determine the angular resolution for the charge-exchange experiment.

The nuclei in brass are about 45% protons and 55% neutrons, so that about 10% of the total number of annihilations are possibly different for calibrations and data, being $\bar{p}n$ for antiprotons incident and $\bar{n}n$ for antineutrons. These annihilation cross sections are very similar, and the small effect of the net charge difference for the two types of annihilation is minimized by the

[8] A. S. Carroll, J. Fischer, A. Lundby, R. H. Phillips, C. L. Wang, F. Lobkowicz, A. C. Melissinos, Y. Nagashima, C. A. Smith, and S. Tewksbury, Phys. Rev. Letters **21**, 1282 (1968).

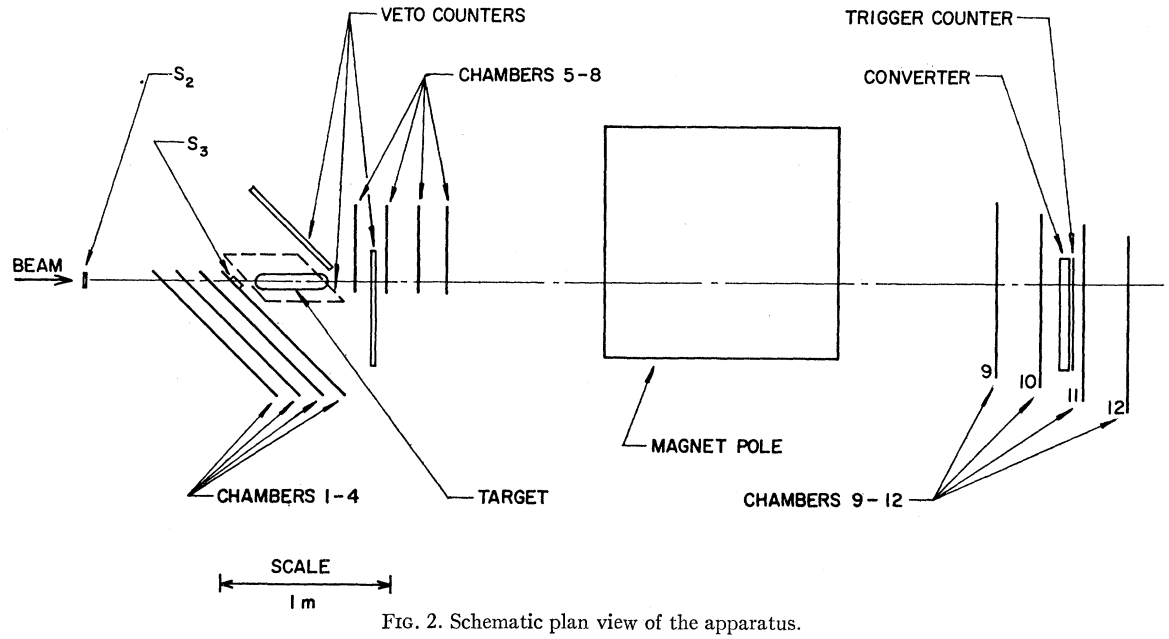

FIG. 2. Schematic plan view of the apparatus.

fact that many π^0 photons are converted to pairs in the converter. The multiplicity of charged particles in the experiment is thus larger than in simple annihilations. We therefore anticipate that the asymmetry in antiproton and antineutron interactions in the converter will at worst lead to a small normalization error, less than a few percent.

In order to calibrate the apparatus with antiprotons, the magnet was turned off and the antiproton beam was allowed to strike the converter. Beam particles were selected which had coordinates in chambers 9 and 10 that were consistent within measurement errors with an extrapolation of the trajectory from chambers 1–4. The tracks in chambers 9 and 10 which were ascribed to the beam particle were then "erased," in that they were removed from further analysis.

Events were rejected if they had a track after the converter within a 3° cone of the incident antiproton direction, as seen in chamber 12. This effectively rejected small-angle elastic-scattering events, as well as noninteracting antiprotons, and introduced a very small loss of annihilation events.

The results of the calibration data were analyzed in terms of numbers of forward and backward tracks, detected in spark chambers 10 and 11, for each interaction. (Chambers 9 and 12 were useful for tests, but subtended too small a solid angle at the converter for unbiased data collection.) In order to minimize effects from multispark inefficiencies, the number of tracks was essentially taken to be the larger of the numbers of sparks in either coordinate of a given chamber. The calibration data were then sorted into 16 topologies determined by the number of forward and backward tracks, and numbered as shown in Fig. 3.

The electronics for the wire chambers actually limited the total number of detected sparks to a maximum of four per chamber, so that the column for four forward tracks includes greater than four, and that for three back tracks similarly includes greater than three. (The back-track capacity for calibrations is reduced by one because of the incident, and later erased, antiproton track.) The diagonals of the matrix, shown by dotted lines in Fig. 3(b), correspond to increasing total numbers of tracks, and the percentage of events in each diagonal is shown in the table on the figure. A

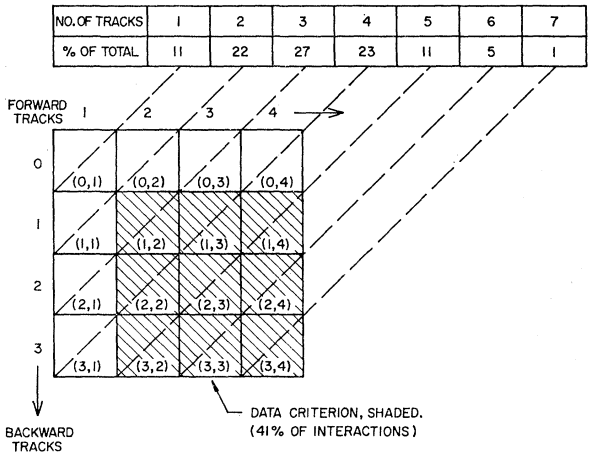

FIG. 3. Topologies for annihilations in the brass converter. The number pairs in the matrix identify various combinations of forward and backward track multiplicities. Sums along the diagonals of the matrix are given, for antiproton calibration data, where each diagonal corresponds to a fixed total number of tracks, ranging from 1 to 7.

reasonable detection efficiency can be obtained by requiring three or more tracks for a bona fide event.

Calibration runs were also taken with a π^- beam incident and the normal charge-exchange trigger. These data select γ rays converting in the converter, largely from $\pi^- - p$ charge-exchange scattering. The multiplicity was seen to be high, but only in the forward spark chamber, as might be expected for electromagnetic showers. As a result, events with no backward tracks were ruled out for $\bar{p}p$ charge-exchange data.

The final criterion for an antiparticle annihilation was chosen to correspond to the shaded area shown in Fig. 3. Events with a single forward track were rejected, as well as those with no back track. This criterion includes $(41\pm1)\%$ of all antiproton calibration interactions, and interactions occurred for $(44\pm1)\%$ of the antiprotons incident on the converter. The over-all efficiency for antiproton detection, taken to be the same for antineutrons, was therefore $(18.0\pm0.7)\%$.

The calibration data also yield a measure of the error in determining the coordinates of an annihilation, which leads to an error in antineutron angle. For each calibration interaction the true x and y coordinates (in the plane perpendicular to the beam direction) are accurately known from the antiproton tracks in chambers 9 and 10. These may be compared with the estimated location of the interaction from the average of the spark coordinates in chamber 11. The difference is found to approximately exhibit a Gaussian distribution, with a standard deviation of ±3.5 cm for either the horizontal or vertical coordinate.

The angular measurement for a charge-exchange event also has an uncertainty because of the error in the incident antiproton angle at the target. This was studied with the calibration data by comparing measured trajectories in chambers 9 and 10 with extrapolated trajectories from the chambers preceding the target. The effect of this uncertainty was found to be small compared with the positional uncertainty in the converter. The net uncertainty in laboratory angle varies from about $\pm0.8°$ at $\theta=0°$ to $\pm0.5°$ for θ greater than 2°. (For the larger angles, only the uncertainty in one coordinate influences the angular uncertainty.) The data have been collected in 1° bins and, considering the way in which the cross section varies, this angular inaccuracy introduces negligible error.

C. Corrections

Figure 4 shows the distribution of events among the various converter topologies for antiproton calibrations and for the events recorded during the $\bar{p}p$ charge-exchange runs. The antiproton calibrations were interspersed among the data runs to guard against sys-

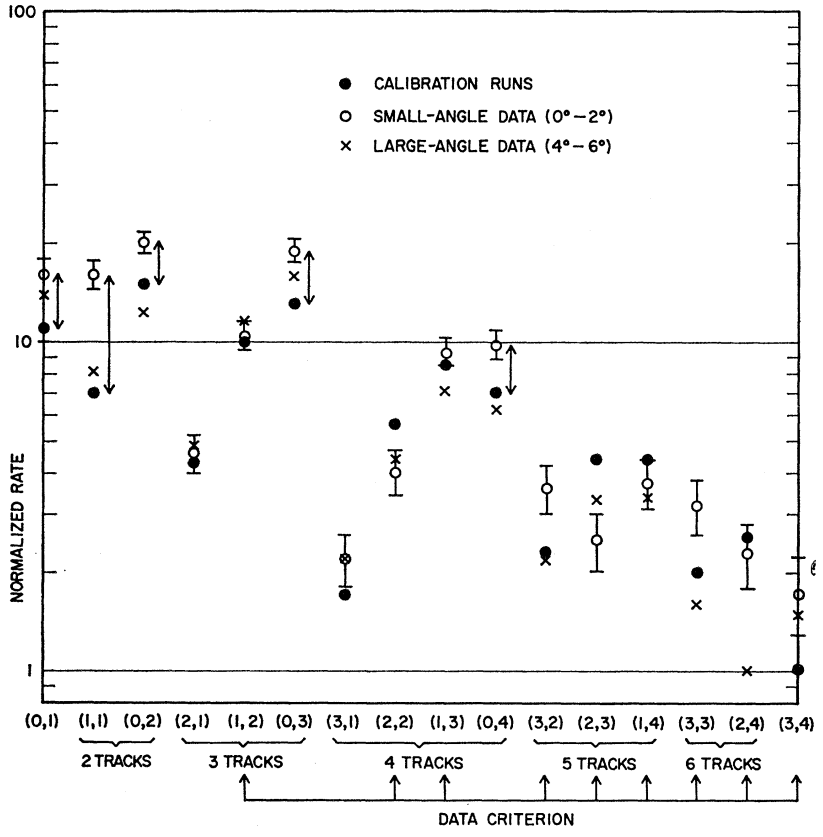

FIG. 4. Data and calibration rates for various topologies. Statistical errors, shown only for the small-angle data, are also appropriate for the large-angle data and calibration runs. Vertical arrows indicate background inferred for the small-angle data. Large-angle data are shown with this background subtracted.

tematic shifts with time. The solid circles are the calibration data, in percent of antiproton interactions, while the open circles are the topology distribution for the charge-exchange events which occurred near 0°, in the region where the calibration antiprotons hit the converter. Statistical errors are shown for the open circles, and the errors for the calibration data and for the large-angle charge-exchange data are not very different and have been left off the figure for clarity.

The small-angle charge-exchange data shown in Fig. 4 have been normalized so that the integrated rate for the criterion corresponding to the shaded region of the matrix in Fig. 3 is the same for the data and for the antiproton calibrations. When this is done, the relative rates for most of the different topologies agree with the antiproton calibration, except for topologies (0,1), (0,2), (0,3), (0,4), and (1,1). The excess in these topologies is indicated with arrows in Fig. 4, and is interpreted as background from γ rays [(0,1), (0,2), (0,3), and (0.4)], and from stray charged particles, (1,1).

The topology comparison between the calibrations and the data represents our only check that solely antineutron interactions are being detected in the data runs. A background, consisting of the excess noted above for topologies not used for data collection, was assumed to be constant over the small solid angle of the converter. For the larger-angle data, the points labeled × on Fig. 4 show that after this background is subtracted the topologies are also in good agreement with the antiproton calibration.

We have been particularly interested in checking whether there is an angle-dependent bias introduced in the data by a variation in spark-chamber performance over the area of the converter. Calibration data were not used to check this, and the only check we have is the comparison between the large-angle data and the calibrations, shown in Fig. 4. After background subtraction, the fraction of the total events which is encompassed by the data criterion is $(37\pm1.5)\%$ compared to $(41\pm1.5)\%$ for calibrations. Most of this difference can be ascribed to a low rate for high-multiplicity events.

In view of the comparison above, and some other evidence for deterioration of the multispark efficiencies of the spark chamber in the large-angle region, the data have been corrected for a net bias of up to 10%, taken to be linearly increasing at 2% per degree. The uncertainty in this correction is estimated at about half of itself, $\pm5\%$ at the large angles.

A further source of error is the possibility that the slow recoil neutron is counted by a veto counter. The report by Kurz[9] has been used to estimate the counter efficiency. Neutrons with energy below about 2 MeV would not be counted, while recoils with energy >2 MeV would have to be counted in one particular veto counter, to the left of the target, made of $\frac{1}{4}$-in.-thick plastic scintillator. The neutron efficiency of this counter is estimated to rise with increasing $|t|$ to a maximum of $2\frac{1}{2}\%$ at $|t|$ about 0.012 $(\mathrm{GeV}/c)^2$ and to then fall slowly to 1.6% at $|t|=0.03$ $(\mathrm{GeV}/c)^2$ which corresponds to the largest value of θ for this experiment. The data have been corrected for this effect, estimated to be known with an accuracy equal to the correction.

Data were accepted in which the x and y averages of spark coordinates in chamber 11 fell within a region $2\frac{1}{2}$ cm inside the top and bottom edges of the converter, 8 cm in from the left edge, and 5 cm in from the right edge. As a result of the 3.5-cm standard error in coordinate estimates there was a net event loss because of the finite converter size. The correction was calculated and applied to the data for each of the 1° bins, and was about 9% in all cases.

Finally, the data were corrected for losses resulting from interactions of the beam antiprotons and the produced antineutrons. A total cross section of 95 mb, taken from the data of Abrams *et al.*,[10] was used for both antiprotons and antineutrons. Interactions in the hydrogen target and in the other material along the beam line were considered (taken proportional to $A^{2/3}$), and a net correction factor of 1.25 was determined.

III. RESULTS AND DISCUSSION

Table I lists the differential cross sections measured in this experiment, with the purely statistical errors. In addition, an estimated systematic error is given, which is correlated from point to point, and represents the uncertainty in angle-dependent corrections for spark-chamber inefficiencies and neutron detection in the veto counters. We also estimate an over-all normalization error of about $\pm5\%$, dominated by uncertainty in the antineutron detection efficiency.

The data are plotted in Fig. 5, with statistical errors only, and compared with extrapolations from np charge-exchange experiments at 1.36 and 3.0 GeV/c.[3,4] These np data have been scaled to 1.80 GeV/c by assuming that the t dependence is unchanged and that the total cross section varies as $(1/p_{\mathrm{lab}})^2$. The two sets of np data extrapolated in this way are seen to be in good

TABLE I. Measured cross sections.

θ_{lab} (deg)	t $(\mathrm{GeV}/c)^2$	$d\sigma/dt$ [mb/$(\mathrm{GeV}/c)^2$]	Systematic error [mb/$(\mathrm{GeV}/c)^2$]
0.7	0.0005	27.7±2.0	±0.1
1.5	0.0022	26.9±1.7	±0.3
2.5	0.0061	24.3±1.7	±0.5
3.5	0.012	23.4±1.6	±0.7
4.5	0.020	18.3±1.5	±0.8
5.5	0.030	16.7±1.5	±0.9

[9] R. J. Kurz, LRL Report No. UCRL-10564 (unpublished).

[10] R. J. Abrams, R. L. Cool, G. Giacomelli, T. F. Kycia, B. A. Leontic, K. K. Li, and D. N. Michael, Phys. Rev. Letters 18, 1209 (1967).

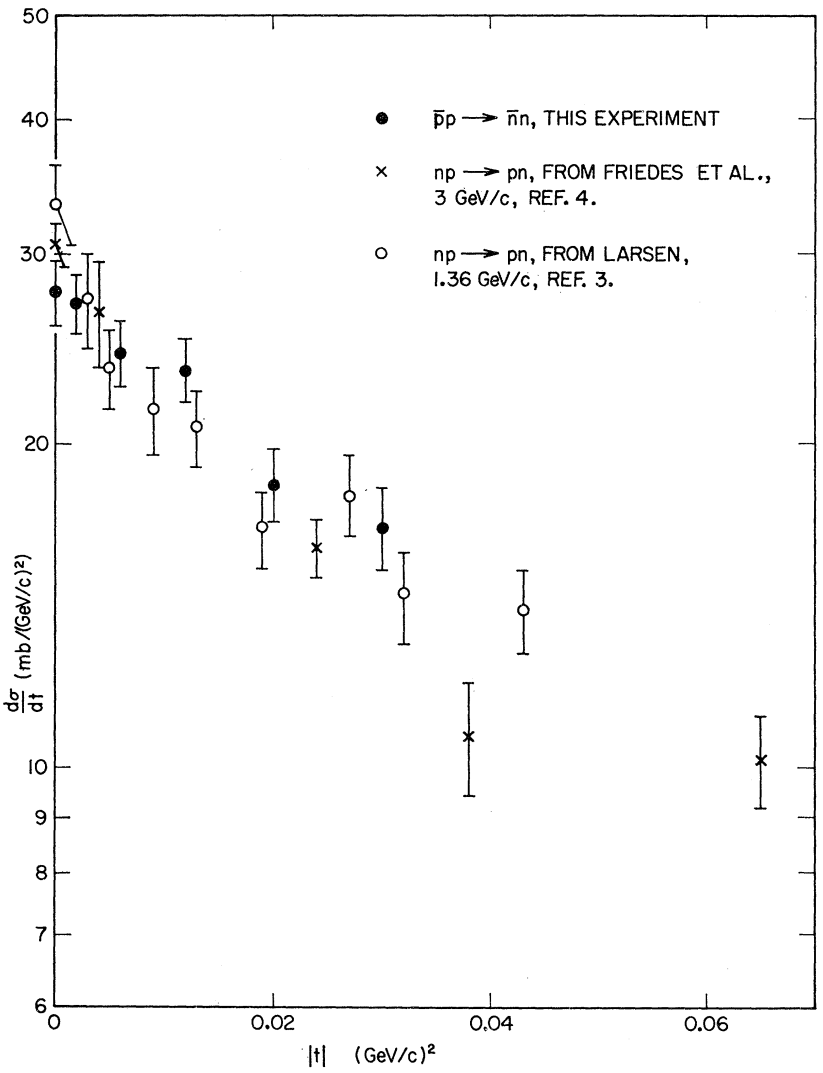

FIG. 5. Results of this experiment and of np charge-exchange experiments. The errors shown are purely statistical, and the np data are scaled as $(1/p_{\text{lab}})^2$.

agreement, and these data are also consistent with the results of Mischke *et al.*[6] at 1.74 GeV/c.

The $\bar{p}p$ charge-exchange cross sections shown in Fig. 5 are quite similar to the np cross sections. However, the total $\bar{p}p$ charge-exchange cross section, determined at 1.61 GeV/c by Hinrichs *et al.*,[7] is about 1.5 times the total np charge-exchange cross section. Thus, for $|t| > m_\pi^2$, the $\bar{p}p$ charge-exchange cross section must be considerably larger than the np cross section, as has been directly observed at higher energies.[11,12] The qualitative result of this experiment, when combined with the total-cross-section data, is thus that there is a forward peak in the $\bar{p}p$ charge-exchange cross section, but that it is relatively less important than the similar peak in the np cross section.

To express the result more quantitatively, Table II shows the observed cross sections $(d\sigma/dt)_{t=0}$ and estimates of the contributions to these cross sections, $(d\sigma/dt)_\pi$, from a sharp forward peak at $|t| \lesssim m_\pi^2$. The contribution $(d\sigma/dt)_\pi$ has been found by subtracting from the measured cross section an amount $(d\sigma/dt)_{\text{ext}}$, extrapolated from a fit of the form $Ae^{-B|t|}$ to the cross section for $|t|$ larger than 0.1 (GeV/c)². For the np data

TABLE II. Differential cross sections at zero degrees for charge-exchange scattering. The three columns give, successively, the observed cross sections $(d\sigma/dt)_{t=0}$; estimates of extrapolated cross sections without sharp forward peaking, $(d\sigma/dt)_{\text{ext}}$; and the contribution of the forward peak, $(d\sigma/dt)_\pi$.

	$(d\sigma/dt)_{t=0}$ [mb/(GeV/c)²]	$(d\sigma/dt)_{\text{ext}}$ [mb/(GeV/c)²]	$(d\sigma/dt)_\pi$ [mb/(GeV/c)²]
np	32±3	12 ±2	20 ±3.5
$\bar{p}p$	28±2	22.5±3.5	5.5±4

[11] O. Czyzewski, B. Escoubes, Y. Goldschmidt-Clermont, M. Guinea-Moorhead, D. R. O. Morrison, and S. De Unamuno-Escoubes, Phys. Letters **20**, 554 (1966).

[12] P. Astbury, G. Brautti, G. Finocchiaro, A. Michelini, D. Websdale, C. H. West, E. Polgar, W. Beusch, W. E. Fischer, B. Gobbi, and M. Pepin, Phys. Letters **22**, 537 (1966); **23**, 160 (1966).

a fit of this form for data[4] at 3.0 GeV/c was extrapolated to our momentum, assuming that the parameter B remains unchanged.

In order to find $(d\sigma/dt)_{\text{ext}}$ for $\bar{p}p$ charge exchange, the parameter B in the exponential fit has been taken to be 4.5 ± 0.5 $(\text{GeV}/c)^{-2}$, from data at higher momenta.[11,12] From the data of Hinrichs *et al.*,[7] the total cross section, scaled to 1.80 GeV/c, has been estimated to be 5.0 ± 0.6 mb. Scaling according to $(1/p_{\text{lab}})^2$ has been used, consistent with the data collected in Ref. 12. The parameter A has been estimated to be 22.5 ± 3.5 mb/$(\text{GeV}/c)^2$ by requiring that the total cross section be given by the Ae^{-Bt} fit.

If we interpret the incremental cross sections $(d\sigma/dt)_\pi$ as the result of pion exchange, there must be interference with an exchange of opposite G parity. Such an interference must contribute half the difference of the two incremental cross sections, or about 7 mb/$(\text{GeV}/c)^2$. Since the pion can only interfere with t-channel exchanges which have the product $PG=+1$,[13] an obvious candidate for the needed interference is the B meson. Interference with odd G-parity exchanges, plus the square of the pion exchange amplitude, must add up to half the sum of the two incremental cross sections, or about 13 mb/$(\text{GeV}/c)^2$. From the available data, it is not possible to separate these two contributions.[14]

There have been numerous theoretical papers discussing the forward np charge exchange, some of which also have made predictions for the $\bar{p}p$ charge exchange. Geicke and Mutter have fit the data with three Regge poles, including π and B mesons,[15] and their results appear to be in fair agreement with the data of this experiment. Other theoretical papers have predicted $\bar{p}p$ charge-exchange cross sections inconsistent with our results.[13,16] The forward $\bar{p}p$ charge-exchange data add important constraints to fits involving pion exchange, and better data, covering more angles and a wider range of energies, will be helpful in evaluating the theoretical pictures which have been suggested.

ACKNOWLEDGMENTS

We would like to acknowledge the invaluable assistance of Hans Grau in setting up this experiment. We also want to thank Professor Steven Frautschi for helpful discussions.

[13] K. Huang and I. J. Muzinich, Phys. Rev. **164**, 1726 (1967).

[14] Although they are not unique, we find that interference between exchange amplitudes which vary as e^{-2t} and e^{-25t} give a good representation of the cross sections. The fits to the $\bar{p}p\to\bar{n}n$ and $np\to pn$ cross section are $19e^{-4t}+15e^{-50t}-6e^{-27t}$ and $11e^{-4t}+15e^{-50t}+6e^{-27t}$, respectively.

[15] J. Geicke and K. H. Mütter, Phys. Rev. **184**, 1551 (1969).

[16] P. R. Graves-Morris, Phys. Rev. **181**, 1940 (1969).

PHYSICAL REVIEW D VOLUME 2, NUMBER 11 1 DECEMBER 1970

Search for Doubly Charged Mesons in $\bar{p}p$ Annihilations into Pions near 1.9 GeV/c*

J. LYS AND J. W. CHAPMAN
The University of Michigan, Ann Arbor, Michigan 48104
(Received 29 June 1970)

We have searched for evidence of doubly charged mesons in 45 000 events of the type $\bar{p}p\to\pi^+\pi^+\pi^-\pi^-+n\pi^0$, $n\geq0$, at incident antiproton momenta 1.6–2.2 GeV/c. We find no evidence for such mesons, and give upper limits for production cross sections.

INTRODUCTION

A STRIKING feature of resonance spectroscopy in high-energy physics is the apparent absence of meson resonances with isospin greater than one.[1] Such meson resonances cannot be formed by a quark-antiquark ($q\bar{q}$) pair in the quark model, and hence belong to that class of states generally referred to as exotic. A recent review of some of the theoretical implications of the absence of exotic resonances has been given by Lipkin.[2] It is clearly important to get experimental upper limits on production cross sections for possible exotic resonances in various reactions.

There is an additional reason for looking for exotic mesons in an antiproton-proton experiment. It has been pointed out[3] that a strict application of the concept of duality to baryon-antibaryon scattering requires the existence of certain exotic mesons. In terms of quarks and antiquarks, if the t-channel exchanges involve single $q\bar{q}$ pairs, then the s-channel states that build these exchanges must be $qq\bar{q}\bar{q}$. A selection rule, inspired by the quark model, has been suggested[4] which reduces to well-known rules for the couplings of nonexotic mesons and

* Work supported by the U.S. Atomic Energy Commission.

[1] Particle Data Group, Rev. Mod. Phys. **42**, 87 (1970).

[2] H. J. Lipkin, in *Proceedings of the Boulder Conference on High-Energy Physics* (Colorado Associated U. P., Boulder, Colo., 1970), p. 386.

[3] J. Rosner, Phys. Rev. Letters **21**, 950 (1968).

[4] P. Freund, R. Waltz, J. Rosner, Nucl. Phys. **B13**, 237 (1969).